Available online at www.sciencedirect.com
ScienceDirect
Biochemical and Biophysical Research Communications 348 (2006) 124–131
BBRC
www.elsevier.com/locate/ybbrc

Role of metal-binding domains of the copper pump from *Archaeoglobus fulgidus* ☆

William J. Rice [a,b,*], Aleksandra Kovalishin [a], David L. Stokes [a,b]

[a] *Skirball Institute of Biomolecular Medicine, New York University School of Medicine, New York, NY 10016, USA*
[b] *New York Structural Biology Center, New York, NY 10027, USA*

Received 29 June 2006
Available online 13 July 2006

Abstract

CopA from the extreme thermophile *Archaeoglobus fulgidus* is a P-type ATPase that transports Cu^+ and Ag^+ and has individual metal-binding domains (MBDs) at both N- and C-termini. We expressed and purified full-length CopA as well as constructs with MBDs deleted either individually or collectively. Cu^+ and Ag^+-dependent ATPase assays showed that full-length CopA had submicromolar affinity for both ions, but was inhibited by concentrations above 1 μM. Deletion of both MBDs had no effect on affinity but resulted in loss of this inhibition. Individual deletions implicated the N-terminal MBD in causing the inhibition at concentrations >1 μM. Rates of phosphoenzyme decay indicated that neither the dephosphorylation step, nor the E1P–E2P equilibrium accounted for this inhibition, suggesting the involvement of a different catalytic step. Alternative hypotheses are discussed by which the N-terminal MBD could influence the catalytic activity of CopA.

Keywords: P-type ATPase; CopA; Copper pump; Extremophile; Metal-binding domain; Membrane protein; Thermophile; P1b ATPase

P-type ATPases are a large and diverse group of membrane proteins, that transport a variety of monovalent and divalent cations in bacteria, fungi, plants, and animals [1], and that share a phylogenetic origin [2]. This family is characterized by conserved sequence motifs involved in ATP hydrolysis and by the formation of an acid-stable phosphoenzyme intermediate during the reaction cycle [3]. The majority of family members transport the common ions from the alkali metals and alkaline earth elements such as Na^+, K^+, H^+, Ca^{2+}, and Mg^{2+}, but the P1b subfamily transports transition metal ions such as Cu^+, Ag^+, Cu^{2+}, Zn^{2+}, and Pb^{2+}, which are generally present in trace amounts. While the best characterized P1b pumps come from bacteria [4,5], an increasing number of copper-transporting ATPases are being identified in fungi, plants, and animal cells. With respect to humans, considerable work has been done on two copper-transporting P1b pumps that, when defective, give rise to Menkes and Wilson's diseases (MNK and WNDP, respectively [6]). In many cases, the cellular role of these pumps is simply to maintain low intracellular concentrations of potentially toxic ions, but MNK has been shown to be important not only in absorption of dietary copper from the intestine, but also in delivery of copper to metalloenzymes involved in secretion [7].

The N-terminal tail of P1b pumps contains repeated sequence motifs that appear to be designed to bind metal ions [8]. For pumps with the CPC transport sequence in transmembrane helix 6 (CopA, ZntA, CadA, MNK, and WNDP), the N-terminal tail contains from one to six repeated GxxCxxC motifs. The striking structural similarity between the fourth GxxCxxC repeat of the Menkes protein [9] and small, soluble copper chaperones, such as Atx1 from yeast [10] and CopZ from *Enterococcus hirae* [11],

☆ *Abbreviations:* ΔN, truncated CopA lacking the first N-terminal 95 amino acids; ΔC, truncated CopA lacking the final C-terminal 68 amino acids; ΔNΔC, truncated CopA lacking both the N-terminal 95 and C-terminal 68 amino acids; MBD, metal-binding domain; MNK, Menkes disease pump; WNDP, Wilson's disease pump; DTT, 1,4-dithiothreitol; BCS, bathocuproinedisulfonate; EDTA, ethylenediaminetetraacetic acid; MES, *N*-morpholineodisulfonic acid; Tris, tris(hydroxymethyl)amine.

* Corresponding author. Fax: +1 212 939 0863.
E-mail address: rice@nysbc.org (W.J. Rice).

0006-291X/$ - see front matter © 2006 Elsevier Inc. All rights reserved.
doi:10.1016/j.bbrc.2006.07.012

strongly suggests that these domains bind Cu^+. Indeed, such binding has been confirmed for heterologously expressed, isolated metal-binding domains (MBD) from MNK and WNDP, either by direct-binding assays [12–14] or by chemical labelling of the coordinating cysteines in the presence and absence of metal ions [15]. A role in metal binding has also been postulated for the His-rich domains that comprise the N-terminus of CopB [16,17] and the CCCDGAC motif that has recently been implicated in Pb^{2+} transport by ZntA [18]. Activity measurements on a variety of different pumps have shown relatively subtle effects of mutagenesis or truncation of the GxxCxxC motifs, suggesting that although the MBDs may modulate this activity, they are not absolutely required for transport [15,19–21].

For this study, we have used CopA from *Archaeoglobus fulgidus* to further investigate the functional effects of truncating its MBDs. This pump has, in addition to a single N-terminal MBD, a unique C-terminal domain with a GxxCxxC motif. A previous study showed that mutation of cysteines in the C-terminal MBD had no effect on activity but mutation of cysteines in the N-terminal MBD resulted in a loss of ~50% ATPase activity [21]. For our work, CopA was heterologously expressed in *Escherichia coli* and appeared homogeneous on analytical gel filtration columns. Our protein had much higher levels of ATPase activity and higher affinities than previously reported, was stimulated by submicromolar concentrations of Cu^+ and Ag^+, and was inhibited by these ions at concentrations above 1 μM. Simultaneous deletion of N- and C-terminal MBDs did not adversely affect maximal ATPase activity or ion affinity, but did eliminate the inhibition of ATPase activity at Cu^+ concentrations greater than 1 μM. Selective deletion of either the N- or C-terminus indicated that the N-terminal tail was responsible for this inhibition. Phosphorylation assays showed that inhibition was not caused by slower dephosphorylation at high Cu^+ concentrations or alterations in the E1P–E2P equilibrium, suggesting that a different step in the catalytic cycle was responsible.

Materials and methods

Constructs. Fig. 1A shows diagrammatically the four constructs of CopA used for the current study: (1) full-length sequence (FL), (2) truncation of the N-terminal 95 residues (ΔN), (3) truncation of the C-terminal 68 residues after the last transmembrane helix (ΔC), and (4) truncation of both N- and C-termini (ΔNΔC). The CopA gene was initially cloned by PCR from a genomic DNA library from *A. fulgidus* (ATCC Corp.) and ligated into the pBAD expression vector (Stratagene) between the *Nco*I and *Hin*dIII sites, thus removing the existing N-terminal c-Myc tag and C-terminal His_6 tag included in this vector. Instead, we added the sequence $GTGLVPRGSSH_8$ to the C-terminus of each construct, which provided a His_8 tag preceded by a thrombin cleavage site between Arg and Gly. For N-terminal truncations, the dipeptide MV was added at the N-terminus. The oligonucleotides used for PCR are shown in Table 1.

Expression and purification. For each expression, 60 ml of an overnight culture of *E. coli* (strain LMG1940) was added to 6 L of LB broth with 100 μg/ml ampicillin at 37 °C and was grown to an OD of ~0.6. After reducing the temperature to 30 °C, the culture was grown to an OD of 1.0, at which point expression was induced with 0.002% arabinose. The culture

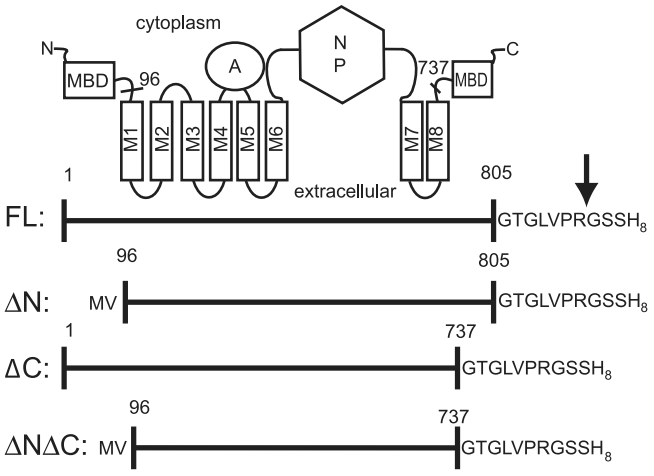

Fig. 1. Schematic representation of CopA showing the four constructs used in this study. The sequence of the C-terminal tag is shown, with an arrow showing the thrombin cleavage site.

was incubated for a further 2 h at 30 °C and then harvested by centrifugation at 7500 rpm for 15 min at 4 °C (Sorvall SLA 3000 rotor). The pellet was suspended in a buffer composed of 25 mM Tris–Cl, pH 7.5, 10% glycerol, 5 mM 2-mercaptoethanol, and 0.05 mg/ml DNAse I; protease inhibitor cocktail was added according to the manufacturer's (Sigma) instructions. Cells were broken by two passages through a French Press operating at 20,000 psi. Cell debris was removed by centrifugation at 7500 rpm for 20 min at 4 °C (Sorvall GS3 rotor). Membranes were collected by centrifugation at 35,000 rpm for 2.5 h at 4 °C (Beckman Ti-45 rotor) then frozen and stored at −80 °C.

Membranes were suspended in 25 mM Tris–Cl, pH 7.5, 100 mM NaCl, 10% glycerol, and 5 mM mercaptoethanol (buffer A) at a protein concentration of 10 mg/ml and solubilized by the addition of 10 mg/ml sol-grade DDM (Anatrace). After gently mixing for 30 min at 4 °C on a rocking platform, insoluble material was removed by centrifugation at 35,000 rpm for 30 min at 4 °C (Beckman Ti-45 rotor). A 5 ml HiTrap Chelating HP column (GE Healthcare) was charged with 100 mM $NiCl_2$ and then washed in buffer A supplemented with 25 mM imidazole and 1 mg/ml DDM. Twenty-five millimolar imidazole was added to the protein supernatant, which was then loaded onto the column at 1 ml/min using a low-pressure chromatography system (BioRad). The column was then washed in buffer A containing 1 mg/ml DDM and a step-wise series of increasing imidazole concentrations: 25 ml at 25 mM imidazole, 15 ml at 50 mM imidazole, and 15 ml at 80 mM imidazole. Purified CopA was eluted with 20 ml of buffer A, 1 mg/ml DDM, and 300 mM imidazole. Pooled fractions were typically 1 mg/ml and, after adding 1 U thrombin per mg of protein, were dialyzed overnight against 25 mM Tris–Cl, pH 7.5, 30 mM NaCl, 10% glycerol, and 5 mM 2-mercaptoethanol. Thrombin was removed by passage over a benzamidine–Sepharose column (GE Healthcare). For concentration, the protein was loaded at 0.25 ml/min onto a HiTrap Q HP column (GE Healthcare) pre-equilibrated with 25 mM Tris–Cl, pH 7.5, 30 mM NaCl, 10% glycerol, 1 mg/ml DDM, and 2.5 mM DTT. This column was then washed with 25 ml of the equilibration buffer and CopA was eluted with the same buffer supplemented with 300 mM NaCl. Peak fractions were collected within the first 3 ml of elution and generally resulted in protein concentrations of 1.5–3 mg/ml. Chloride was exchanged for sulfate by dialysis against two 300 ml changes of 50 mM Tris–SO_4, pH 7.5, 100 mM Na_2SO_4, 5 mM $MgSO_4$, 10% glycerol, 2.5 mM DTT, and 0.008% DDM. Protein concentration was determined by absorbance at 280 nm.

ATPase activity assays. ATPase activity was quantified by measuring phosphate production using the malachite green assay described by Kimura et al. [22]. The assay was conducted in a solution of 50 mM Tris–SO_4, 200 mM Na_2SO_4, 3 mM $MgSO_4$, 5 mM glutathione, 2.4 mM ATP, 10% glycerol, 0.5 mg/ml DDM, 0.025% NaN_3, 0.05 mg/ml bacterial total

Table 1
Oligonucleotides used for vector construction

Construct	5′Oligo	3′Oligo
Full-length	TGCCATGGTAAAGGATACTTATATCTCT	AGGCCGGTACCGCTTCTGAGCTTTGCCTGGT
ΔN	TGATACCATGGTTTCAAGAATGAAAAGGAAGCTCTACGTG	AGGCCGGTACCGCTTCTGAGCTTTGCCTGGT
ΔC	TGCCATGGTAAAGGATACTTATATCTCT	TATCCGGTACCTCCCCTCCTTATCGGAGGAACGTA
ΔNΔC	TGATACCATGGTTTCAAGAATGAAAAGGAAGCTCTACGTG	TATCCGGTACCTCCCCTCCTTATCGGAGGAACGTA

lipid (Avanti), and varying concentrations of either $CuSO_4$, $AgNO_3$ or BCS; the pH of this solution was adjusted to pH 7.5 at room temperature in order to obtain pH 6.3 at the assay temperature of 70 °C. All nonreducing buffers were pretreated with 100 mg/ml chelex for at least 1 h. CopA protein was added at a concentration between 0.02 and 0.04 mg/ml and this reaction mixture was divided into aliquots and stored on ice, where the enzyme is completely inactive. Using a programmable PCR thermocycler (Eppendorf), duplicate 45-μl aliquots of the reaction mixture were heated to 70 °C for 3, 5, 7, and 9 min then cooled to 4 °C to stop the reaction. Phosphate was then quantified in 96-well microtiter plates using a development time of 3 min; absorbance was read at 630 nm. ATPase activity was calculated as micromoles of phosphate released per minute per milligram of CopA protein.

Phosphoenzyme assays. CopA constructs were phosphorylated at room temperature in a buffer containing 25 mM MES, pH 6.3, 200 mM Na_2SO_4, 10% glycerol, 0.05 mg/ml bacterial total lipid, 2.5 mM glutathione, 3 mM $MgSO_4$, 0.2 mg/ml DDM, and 0.05 mg/ml protein. Phosphorylation was initiated with the addition of varying amounts of [γ-^{32}P]ATP and allowed to proceed for 3 min. For measurement of steady-state phosphoenzyme levels, the reaction was then quenched by addition of 0.5 ml of ice-cold 15% trichloroacetic acid. For dephosphorylation experiments, protein was phosphorylated with 50 μM [γ-^{32}P]ATP for 3 min, then either ATP or ADP was added to a final concentration of 3 mM. After various incubation times, the reaction was quenched with ice-cold 15% trichloroacetic acid. After 1 h on ice, precipitated protein was pelleted by centrifugation at 22,000 rpm for 30 min at 4 °C. Pellets were washed four times with 15% trichloroacetic acid, once with water, then resuspended in 1 ml of scintillation solution. Radioactivity was measured the next day. Background ^{32}P levels were determined by replacing CopA enzyme with bovine serum albumin.

Data analysis. Plots of ATPase activity vs. the concentration of Ag^+ or Cu^+ were fit to the function $V_{min} + (V_{max} - V_{min})/(1 + (K_{0.5}/[M])^H)$, where V_{min} is asymptotic minimum, V_{max} is asymptotic maximum, $[M]$ is metal ion concentration, $K_{0.5}$ is metal ion concentration giving half-maximal activity, and H is the Hill coefficient. Plots of phosphoenzyme level vs. ATP concentration were fit to the function $P_{max}[A]/(K_{0.5} + A)$, where P_{max} refers to maximal phosphoenzyme levels, $[A]$ is ATP concentration, and $K_{0.5}$ is the ATP concentration giving half-maximal activity. Plots of phosphoenzyme decay were fit to $P_0e^{(-Bt)}$, where P_0 refers to initial phosphoenzyme levels, t is time, and B is the decay constant. Half lives were calculated as $t_{1/2} = \ln(2)/B$. Curve fitting was performed using SigmaPlot (Systat Software, Richmond CA). The reported standard errors are the asymptotic standard errors reported by this fitting program.

Results

Expression and purification

We prepared four constructs of the gene for CopA from *A. fulgidus* (Fig. 1) and expressed the corresponding protein in *E. coli*. These constructs corresponded to the full-length protein (FL), a truncation of the entire N-terminal tail up to the first transmembrane helix (ΔN), a truncation of the entire C-terminal tail after the last transmembrane helix (ΔC), and truncation of both N-terminal and C-terminal tails (ΔNΔC). The constructs all contained 8×-His tags at the C-terminus that were used for purification and subsequently removed by proteolysis. Expression levels for all four constructs were quite high, producing a final yield of 6–9 mg of purified protein from 6 L of bacterial expression media. SDS–PAGE showed that the preparations were >95% pure and gel filtration showed that each of the preparations was homogeneous, thus representing excellent candidates for future crystallization trials (Fig. 2).

ATPase assays

As a first step in characterizing our full-length CopA construct, we measured the dependence of ATPase activity

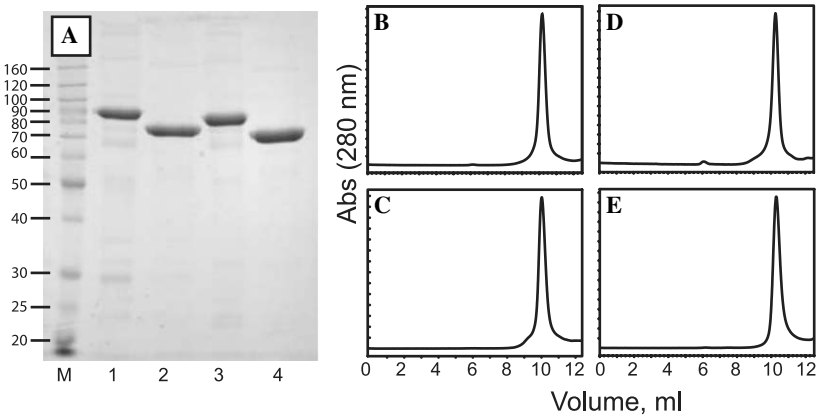

Fig. 2. Preparations of CopA used in this study. (A) Coomassie blue-stained polyacrylamide gel. Lane M contains molecular weight markers with lanes 1–4 containing full-length, ΔN, ΔC, and ΔNΔC constructs of CopA, respectively. (B–E) HPLC chromatograms of purified CopA constructs eluted from a Shodex KW-804 gel filtration HPLC column run at 0.5 ml/min and monitored by UV absorbance at 280 nm. (B–E) Full-length, ΔN, ΔC, and ΔNΔC constructs of CopA, respectively.

of the detergent-solubilized, full-length enzyme on both Cu^+ and Ag^+ concentration (Figs. 3A and B). The assays were conducted at 70 °C, which was previously shown to be optimal for this pump from the thermophile *A. fulgidus* [23]. In the absence of metal ion chelators, we observed a significant level of background ATPase activity (~0.3 μmol/mg/min), presumably due to low levels of Cu^+ contamination in our buffers. Addition of 0.125 mM BCS decreased this background activity twofold and was therefore included when testing the effects of Ag^+ on CopA activity (e.g., Fig. 3B). Cu(I) has been reported as the substrate for CopA and we therefore tested the effect of different reducing agents on the Cu-stimulated ATPase activity. On the one hand, addition of either 2-mercaptoethanol or DTT failed to produce any stimulation in the presence of Cu^+, though baseline activities were unchanged (data not shown). On the other hand, we observed a robust Cu^+-dependent stimulation of ATPase activity in the presence of glutathione, which was therefore included for all the measurements represented in Fig. 3. Data for full-length CopA suggest apparent affinities of 0.26 μM for Cu^+ and 0.55 μM for Ag^+; maximal activities were 1.3 μmol/mg/min in Cu^+ and 1.4 μmol/mg/min in Ag^+ and were reached at 0.8 and 1.0 μM, respectively. Concentrations greater than 1 μM of either ion produced substantial inhibition: Cu^+ produced inhibition at somewhat lower concentrations than Ag^+, though this difference was minimal when Ag^+-dependent assays were conducted in the absence of BCS (data not shown). At 10 μm Cu^+, ATPase activity actually fell below baseline. The data from the rising part of the curve were best fit by a cooperative-binding model and the corresponding Hill coefficients are listed in Tables 2 and 3 together with other kinetic parameters.

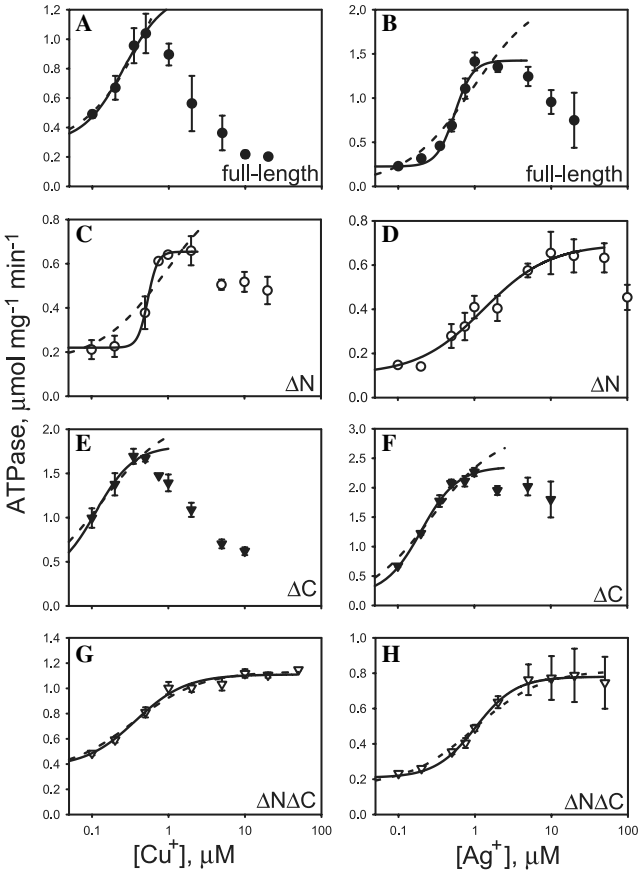

Fig. 3. Cu^+ and Ag^+ dependence of ATPase activities of CopA constructs. (A, C, E, and G) Cu^+-dependent activities. (B, D, F, and H) Ag^+-dependent activities. (A,B) Full-length, (C,D) ΔN, (E,F) ΔC, (G,H) ΔNΔC constructs of CopA. Data points represent mean ± standard error of 3–5 experiments which have been fit to Michaelis–Menten binding model (dashed line) or to the Hill equation (solid line); fitting parameters are listed in Tables 2 and 3.

In order to assess the role of the N- and C-terminal domains of CopA, we performed these same ion-dependent ATPase assays with ΔN, ΔC, and ΔNΔC constructs. Deletion of both N- and C-termini did not have statistically significant effects on apparent ion affinity or V_{max} measured from the rising part of the curves in Figs. 3G and H (Tables 2 and 3). However, ΔNΔC constructs were not inhibited at high concentrations of either Cu^+ or Ag^+.

Individual truncations of N- and C-termini showed intermediate results. Ion affinities were similar, though the ΔN construct was generally closer to ΔNΔC and ΔC was closer to the full-length construct. Similarly, V_{max} for both ΔN and ΔNΔC constructs were moderately lower than that of full-length CopA whereas V_{max} for the ΔC construct was moderately higher. Finally, high ion concentrations inhibited the ΔC construct more than ΔN. Taken together, these results indicate that the ΔC construct is more like full-length CopA and that ΔN resembles ΔNΔC, suggesting that the inhibition of CopA by high Cu^+ concentrations is mediated by the N-terminal tail.

Phosphoenzyme assays

Previous work suggested the dephosphorylation step as a potential point for Cu^+-dependent regulation of CopA [21]. We therefore measured rates of phosphoenzyme decay for our constructs to see if inhibition at high Cu^+ concentrations could be attributed to this dephosphorylation step. Initially, we measured the ATP dependence of phosphoenzyme formation (Fig. 4) and found that all four constructs had a similar affinity for ATP (2–3 μM, Table 4), thus assuring a fair comparison for the dephosphorylation experiments. To measure dephosphorylation in the forward direction (i.e., hydrolysis of E2P), we phosphorylated the enzyme to a steady-state level, then added excess, unlabelled ATP and followed the subsequent phosphoenzyme decay. These experiments were done at two different Cu^+ concentrations corresponding to $K_{0.5}$ from Table 2, which produced half the maximal ATPase activity (Fig. 5A), and to a saturating concentration of 10 μM (Fig. 5B), which produces the maximal inhibition seen in Fig. 3. Half-lives for phosphoenzyme decay are listed in Table 4. Although both full-length and ΔC constructs had significantly lower ATPase activities at the higher Cu^+ concentrations, the decay constants were not significantly different.

Table 2
Kinetic parameters for Cu^+ stimulated ATPase activity of CopA[a]

Construct	$K_{0.5}$ (μM)	V_{max} (μmol/mg/min)	V_{min} (μmol/mg/min)	Hill coefficient
Full-length	0.26 ± 0.13	1.3 ± 0.4	0.29 ± 0.05	1.6
ΔN	0.54 ± 0.01	0.65 ± 0.01	0.22 ± 0.01	6.7
ΔC	0.11 ± 0.02	1.8 ± 0.2	0.32 ± 0.10	1.8
ΔNΔC	0.37 ± 0.06	1.11 ± 0.02	0.37 ± 0.04	1.3

[a] Parameters used to fit solid lines to data in Figs. 3A, C, E, and G.

Table 3
Kinetic parameters for Ag^+ stimulated ATPase assay of CopA[a]

Construct	$K_{0.5}$ (μM)	V_{max} (μmol/mg/min)	V_{min} (μmol/mg/min)	Hill coefficient
Full-length	0.55 ± 0.05	1.43 ± 0.08	0.22 ± 0.04	3.7
ΔN	1.3 ± 0.4	0.69 ± 0.06	0.11 ± 0.04	1.0
ΔC	0.20 ± 0.02	2.36 ± 0.09	0.18 ± 0.06	1.8
ΔNΔC	1.02 ± 0.08	0.78 ± 0.01	0.21 ± 0.02	1.6

[a] Parameters used to fit solid lines to data in Figs. 3B, D, F, and H.

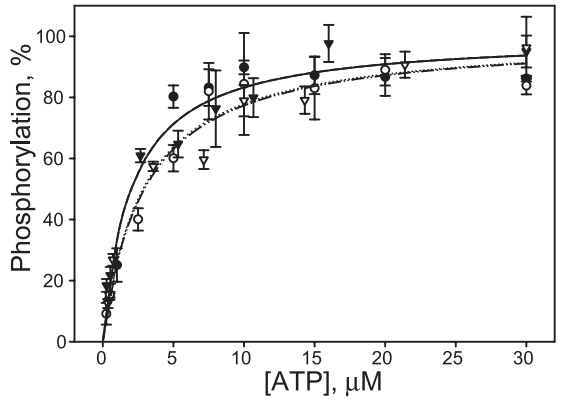

Fig. 4. ATP dependence of phosphoenzyme formation. Data represent means ± standard error for three measurements and were fit to a Michaelis–Menten binding model as described in Materials and methods; fitting parameters are listed in Table 4. Data from Full-length (●, solid line), ΔN (○, dotted line), ΔC (▼, short dashed line), and ΔNΔC (▽, dotted dash line) constructs of CopA are shown. 100% phosphoenzyme formation corresponds to 1.3 nmol phosphoenzyme per mg of protein.

Furthermore, full-length and Δ C constructs were indistinguishable from ΔN and ΔNΔC, which showed little or no inhibition at 10 μM Cu^+.

We then measured the combined phosphoenzyme decay from the forward (hydrolysis of E2P) and reverse (synthesis of ATP from E1P) directions by adding excess unlabelled ADP to steady-state, phosphorylated enzyme. Under these conditions, the fraction of CopA in the E1P state can phosphorylate ADP, thus operating in the reverse direction. The pool of phosphoenzyme in the E2P state is unreactive to ADP, but will hydrolyze to form E2 and P_i. The large excess of added ADP minimizes formation of additional phosphoenzyme. Thus, this experiment reports on the steady-state populations of E1P and E2P and thereby indirectly probes any changes in the rate-limiting step that interconverts these two species. Again, experiments were performed at Cu^+ concentrations corresponding to $K_{0.5}$ and at 10 μM (Figs. 5C and D, respectively). As expected, this combined dephosphorylation was much faster than simple, forward dephosphorylation (Table 4). There is little difference in rates measured for the four constructs, except for a twofold decrease for the full-length construct at high Cu^+ concentration. However, the relatively poor time resolution of our assay makes the significance of this decrease questionable. Furthermore, because this twofold decrease is not reproduced in the ΔC construct, we conclude that the E1P–E2P equilibrium is probably not responsible for the inhibition at high Cu^+ concentrations.

Table 4
Kinetic parameters for phosphorylation and dephosphorylation of CopA

Construct (μM)	K_m[a]	$t_{1/2}$ for ATP[b] $[Cu^+] = K_{0.5}$ (s)	$t_{1/2}$ for ATP[c] $[Cu^+] = 10$ μM (s)	$t_{1/2}$ for ADP[d] $[Cu^+] = K_{0.5}$ (s)	$t_{1/2}$ for ADP[e] $[Cu^+] = 10$ μM (s)
Full-length	2.0 ± 0.6	23	25	4.4	8.8
ΔN	2.8 ± 0.7	30	25	4.6	4.8
ΔC	2.0 ± 0.5	15	22	3.8	4.4
ΔNΔC	2.9 ± 0.8	22	18	5.5	3.7

[a] Parameters for phosphorylation with ATP used to fit data in Fig. 4.
[b] Parameters for dephosphorylation of E2P used to fit data in Fig. 5A.
[c] Parameters for dephosphorylation of E2P used to fit data in Fig. 5B.
[d] Parameters for combined phosphoenzyme decay of E1P and E2P used to fit data in Fig. 5C.
[e] Parameters for combined phosphoenzyme decay of E1P and E2P used to fit data in Fig. 5D.

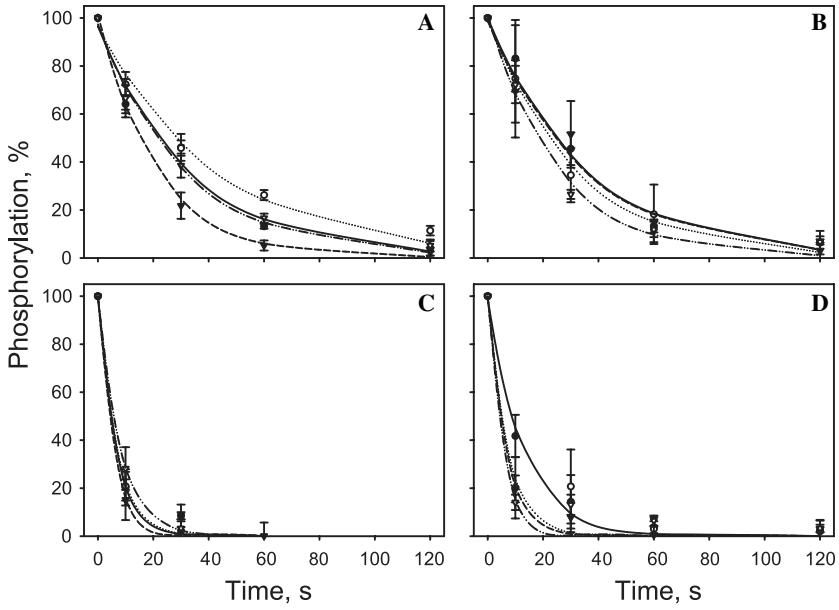

Fig. 5. Phosphoenzyme decay of CopA. Constructs were reacted with [γ-^{32}P]ATP for 3 min at room temperature at two different Cu^+ concentrations, and then treated as follows. (A) Dephosphorylation after addition of 3 mM cold ATP at a Cu^+ concentration corresponding to $K_{0.5}$ indicated in Table 2. (B) Dephosphorylation after addition of 3 mM cold ATP at 10 μM Cu^+. (C) Dephosphorylation after addition of 3 mM ADP at a Cu^+ concentration corresponding to the $K_{0.5}$ in Table 2. (D) Dephosphorylation after addition of 3 mM ADP at 10 μM Cu^+. Symbols and lines are as described for Fig. 4, and represent means ± standard error for three experiments.

Discussion

Metal-binding domains are a distinguishing characteristic of P1b ATPases, which have between one and six of these domains at their N-terminus. CopA from *A. fulgidus* is unusual in that it not only contains one MBD at the N-terminus, but also a second at the extreme C-terminus of the protein. In order to study the relative importance of N- and C- terminal MBDs, we expressed and purified full-length CopA and constructs in which the MBDs had been deleted. We found no substantial differences in metal ion-dependent ATPase activity (Fig. 3) or ATP affinity (Fig. 4) upon removal of these domains. Intriguingly, we did find that the full-length enzyme was inhibited by high concentrations of Cu^+ and Ag^+, and that removal of N- and C-terminal MBDs prevented this inhibition (Fig. 3). Removal of only one MBD at a time showed that most of the effect resides in the N-terminal MBD. We went on to test the effects of these truncations on rates of dephosphorylation of E1P and E2P, but found no significant differences in any of our constructs, suggesting that the MBDs must be influencing a different step in the reaction cycle.

Differences from previous studies

Our assays on the full-length CopA produced significantly different results from those previously published [21,23]. Specifically, we found higher apparent affinities for transport ions, higher maximal enzyme activities, and substantial background activities that could not be eliminated with chelators specific for Cu^+. On the other hand, we did find similar affinities for ATP (2 μM vs. previously reported 4 μM) and steady-state phosphoenzyme level (1.3 nmol/mg vs. 1–1.6 nmol/mg).

With regard to ion affinity, we found significantly higher affinities than previous studies for both Cu^+ and Ag^+. In particular, Mandal et al. [23] reported apparent affinities for full-length CopA of 20 μM for Ag^+ and 2 μM for Cu^+ compared to our values of 0.55 μM and 0.26 μM, respectively. One explanation for our higher Ag^+ affinity is our use of SO_4^{2-} as the counterion rather than Cl^-. Since AgCl is insoluble, precipitation may have interfered with previously published assays. We found a roughly twofold higher affinity for Cu^+ than for Ag^+ in all our constructs, but these measurements are likely influenced by background Cu^+ contamination and, given the complications in controlling total Cu^+ concentration (discussed below), may not reflect any real difference.

We observed V_{max} for ATPase activity that was an order of magnitude greater than previously published reports. This difference may have to do with the reductant used for the assay. We found that 2.5 mM glutathione was essential for observing substantial amounts of Cu^+ stimulated activity. When glutathione was replaced with a similar concentration of DTT, we measured an activity of only ~0.2 μmol/mg/min for the full-length CopA and observed no stimulation by Cu^+. This lower V_{max} value is comparable to that observed by Mandal et al. [23], who used DTT for their ATPase assays. When we replaced glutathione with 2.5 mM ascorbate, we observed no ATPase activity at all, despite the ability of ascorbate to produce Cu(I). These observations suggest that not only the redox state, but also the manner in which Cu^+ is complexed, is important for ATPase activity of CopA. In studies of both ZntA

[24] and WNDP [25], addition of cysteine or glutathione thiolates to the assay buffer increased the ATPase activity fourfold or more. However, addition of thiolates also decreased the apparent affinity of these pumps from 5 μM to 100–200 μM.

We observed a persistent background ATPase activity in the absence of added Cu^+, which has also been seen by several other groups [26–28]. We are confident that the ATPase activities come from our enzyme alone because: (i) the enzyme was 95% pure (Fig. 2A); (ii) activity specifically required a sulfhydryl reductant; and (iii) assays were performed at 70 °C which is likely to inactivate any contaminating ATPases. We attribute this background activity to Cu^+ contamination of 0.1–1 μM in our assay solutions. Since we pretreated nonreducing reagents with chelex, this background Cu^+ probably came from reductants (DTT, glutathione) or may have been purified along with the enzyme. The addition of the Cu^+ specific chelator BCS to the medium lowered the background activity about twofold and was therefore used for Ag^+-dependent assays. Nevertheless, 0.125 mM BCS did not completely eliminate the residual ATPase activity, even though BCS is estimated to have a Cu^+ affinity of the order of 10^{-20} M [29]. This observation is consistent with previous work, in which the addition of even 500 μM BCS has been insufficient to completely inactivate other Cu-ATPases [26–28,30,31]. In the specific case of Tsivkovskii et al. [28], a K_i of 50 μM was measured for BCS, which is many orders of magnitude higher than expected. As discussed by Portmann and Solioz [31], Cu^+ forms extremely high affinity complexes with proteins, buffers, and biomolecules, making the concentration of free Cu^+ extremely difficult to control. Thus, studies of Cu-ATPases are at a marked disadvantage relative to, say, studies of Ca^{2+}-ATPase, where EGTA provides an effective means of buffering Ca^{2+} in the physiological range.

Role of metal-binding domains

Two alternative functional roles have previously been hypothesized for the N-terminal MBDs. According to the first hypothesis, these MBDs mediate the exchange of Cu^+ from soluble metallochaperones to the transport sites of the enzyme within the transmembrane domain. The second hypothesis suggests that they serve as Cu^+ sensors to regulate the activity of the enzyme. The first hypothesis is supported by studies demonstrating that MBDs serve as acceptors for metallochaperone-bound Cu^+ [15,32,33]. This transfer therefore represents a very plausible role for MBDs under physiological conditions. However, many studies have also documented that the pumps transport Cu^+ with high affinity *in vitro* in the absence of metallochaperones [19,30,34,35] and MBDs appear to have little influence over this interaction [15,19–21]. We found that truncation of both MBDs changed neither V_{max} nor Cu^+ affinity. The MBDs may, therefore, be necessary only under physiological conditions where all the available copper is bound to metallochaperones [29].

The alternative hypothesis for a regulatory role of MBDs is supported by the documented interaction between the N-terminal MBD and the ATP-binding domain of WNDP. This interaction appears to be Cu^+-dependent, with the Cu^+-free form of the MBD interacting more strongly [36]. The observed inhibition of CopA at high Cu^+ concentrations might be explained if the Cu^+-bound form of the MBD was inhibitory and required >1 μM Cu^+ to establish this inhibitory interaction. However, previous work contradicts this idea, postulating instead that it is the Cu^+-free MBD that established an inhibitory interaction with the ATP domain. Indeed, precedent is established by other P-type ATPases for inhibitory interactions in the absence of ligand, e.g., plasma membrane Ca^{2+}-ATPase [37], sarcoplasmic reticulum Ca^{2+}-ATPase [38], and plant H^+-ATPase [39]. Therefore, a regulatory interaction between the MBDs and the ATP-binding domain does not appear to offer a compelling explanation for the inhibition of CopA at high Cu^+ concentrations.

A third possibility involves an interplay between the N-terminal MBD and the transport sites of CopA. Assuming that MBDs serve to shuttle Cu^+ from metallochaperones to the membrane-bound Cu^+ site(s), some physical association between the Cu^+-loaded MBD and the transport sites should be expected. This exchange could first require the dissociation of the MBD from the N-domain, perhaps instigated by Cu^+ binding, which would then allow the MBD to interact with transport sites. Since truncated forms of CopA (and other P1b ATPases) appear to be fully active *in vitro*, the membrane-bound Cu^+ sites can apparently also be loaded directly with free Cu^+. At high Cu^+ concentrations, the MBDs would become saturated with Cu^+, which could cause the MDB to remain associated with the transport sites and potentially interfere with release of a transported counterion from the E2 state. Such release is a prerequisite to binding of the primary ion (e.g., Cu^+) to the transport sites and initiation of the ATPase cycle. Although no such counterion has yet been described for P1b ATPases, their existence is well characterized for P2 ATPases [1], and they can inhibit these pumps at elevated concentrations. Further experiments will be needed both to establish the existence of counterion transport for P1b ATPases and to explore the effect of saturated MBDs on their release.

Acknowledgments

The authors acknowledge the contributions of Stefan Dröse and Shihua Xu to early phases of this work, which was supported by a grant from the National Institutes of Health (GM56950 to D.L.S.).

References

[1] J.V. Møller, B. Juul, M. Le Maire, Structural organization, ion transport, and energy transduction of P-type ATPases, Biochim. Biophys. Acta 1286 (1996) 1–51.

[2] K.B. Axelsen, M.G. Palmgren, Evolution of substrate specificities in the P-type ATPase superfamily, J. Mol. Evol. 46 (1998) 84–101.
[3] P.L. Pedersen, E. Carafoli, Ion motive ATPases. I. Ubiquity, properties, and significance to cell function, Trends Biochem. Sci. 12 (1987) 146–150.
[4] C. Rensing, M. Ghosh, B.P. Rosen, Families of soft-metal-ion-transporting ATPases, J. Bacteriol. 181 (1999) 5891–5897.
[5] D. Gatti, B. Mitra, B.P. Rosen, *Escherichia coli* soft metal ion-translocating ATPases, J. Biol. Chem. 275 (2000) 34009–34012.
[6] M. DiDonato, B. Sarkar, Copper transport and its alterations in Menkes and Wilson diseases, Biochim. Biophys. Acta 1360 (1997) 3–16.
[7] M.J. Petris, D. Strausak, J.F. Mercer, The Menkes copper transporter is required for the activation of tyrosinase, Hum. Mol. Genet. 9 (2000) 2845–2851.
[8] M. Solioz, C. Vulpe, CPx-type ATPases: a class of P-type ATPases that pump heavy metals, Trends Biochem. Sci. 21 (1996) 237–241.
[9] J. Gitschier, B. Moffat, D. Reilly, W.I. Wood, W.J. Fairbrother, Solution structure of the fourth metal-binding domain from the Menkes copper-transporting ATPase, Nat. Struct. Biol. 5 (1998) 47–54.
[10] A.C. Rosenzweig, D.L. Huffman, M.Y. Hou, A.K. Wernimont, R.A. Pufahl, T.V. O'Halloran, Crystal structure of the Atx1 metallochaperone protein at 1.02 Å resolution, Structure 7 (1999) 605–617.
[11] R. Wimmer, T. Herrmann, M. Solioz, K. Wuthrich, NMR structure and metal interactions of the CopZ copper chaperone, J. Biol. Chem. 274 (1999) 22597–22603.
[12] S. Lutsenko, K. Petrukhin, M.J. Cooper, C.T. Gilliam, J.H. Kaplan, N-terminal domains of human copper-transporting adenosine triphosphatases (the Wilson's and Menkes disease proteins) bind copper selectively in vivo and in vitro with stoichiometry of one copper per metal-binding repeat, J. Biol. Chem. 272 (1997) 18939–18944.
[13] M. DiDonato, S. Narindrasorasak, J.R. Forbes, D.W. Cox, B. Sarkar, Expression, purification, and metal binding properties of the N-terminal domain from the Wilson disease putative copper-transporting ATPase (ATP7B), J. Biol. Chem. 272 (1997) 33279–33282.
[14] P.Y. Jensen, N. Bonander, N. Horn, Z. Tumer, O. Farver, Expression, purification and copper-binding studies of the first metal-binding domain of Menkes protein, Eur. J. Biochem. 264 (1999) 890–896.
[15] J.M. Walker, D. Huster, M. Ralle, C.T. Morgan, N.J. Blackburn, S. Lutsenko, The N-terminal metal-binding site 2 of the Wilson's Disease Protein plays a key role in the transfer of copper from Atox1, J. Biol. Chem. 279 (2004) 15376–15384.
[16] A. Odermatt, H. Suter, R. Krapf, M. Solioz, Primary structure of two P-type ATPases involved in copper homeostasis in *Enterococcus hirae*, J. Biol. Chem. 268 (1993) 12775–12779.
[17] S. Mana-Capelli, A.K. Mandal, J.M. Arguello, *Archaeoglobus fulgidus* CopB is a thermophilic Cu2+-ATPase: functional role of its histidine-rich-N-terminal metal binding domain, J. Biol. Chem. 278 (2003) 40534–40541.
[18] J. Liu, A.J. Stemmler, J. Fatima, B. Mitra, Metal-binding characteristics of the amino-terminal domain of ZntA: binding of lead is different compared to cadmium and zinc, Biochemistry 44 (2005) 5159–5167.
[19] B. Fan, B.P. Rosen, Biochemical characterization of CopA, the *Escherichia coli* Cu(I)-translocating P-type ATPase, J. Biol. Chem. 277 (2002) 46987–46992.
[20] N. Bal, C.C. Wu, P. Catty, F. Guillain, E. Mintz, Cd(2+) and the N-terminal metal-binding domain protect the putative membranous CPC motif of the Cd(2+)-ATPase of *Listeria monocytogenes*, Biochem. J. 369 (2003) 681–685.
[21] A.K. Mandal, J.M. Arguello, Functional roles of metal binding domains of the *Archaeoglobus fulgidus* Cu(+)-ATPase CopA, Biochemistry 42 (2003) 11040–11047.
[22] Y. Kimura, K. Kurzdylowski, M. Tada, D.H. MacLennan, Phospholamban regulates the Ca2+-ATPase through intramembrane interactions, J. Biol. Chem. 271 (1996) 21726–21731.
[23] A.K. Mandal, W.D. Cheung, J.M. Arguello, Characterization of a thermophilic P-type Ag+/Cu+-ATPase from the extremophile *Archaeoglobus fulgidus*, J. Biol. Chem. 277 (2002) 7201–7208.
[24] R. Sharma, C. Rensing, B.P. Rosen, B. Mitra, The ATP hydrolytic activity of purified ZntA, a Pb(II)/Cd(II)/Zn(II)-translocating ATPase from *Escherichia coli*, J. Biol. Chem. 275 (2000) 3873–3878.
[25] Z.J. Hou, S. Narindrasorasak, B. Bhushan, B. Sarkar, B. Mitra, Functional analysis of chimeric proteins of the Wilson Cu(I)-ATPase (ATP7B) and ZntA, a Pb(II)/Zn(II)/Cd(II)-ATPase from *Escherichia coli*, J. Biol. Chem. 276 (2001) 40858–40863.
[26] J. Lowe, A. Vieyra, P. Catty, F. Guillain, E. Mintz, M. Cuillel, A mutational study in the transmembrane domain of Ccc2p, the yeast Cu(I)-ATPase, shows different roles for each Cys-Pro-Cys cysteine, J. Biol. Chem. 279 (2004) 25986–25994.
[27] H. Wunderli-Ye, M. Solioz, Purification and functional analysis of the copper ATPase CopA of *Enterococcus hirae*, Biochem. Biophys. Res. Commun. 280 (2001) 713–719.
[28] R. Tsivkovskii, J.F. Eisses, J.H. Kaplan, S. Lutsenko, Functional properties of the copper-transporting ATPase ATP7B (the Wilson's disease protein) expressed in insect cells, J. Biol. Chem. 277 (2002) 976–983.
[29] T.D. Rae, P.J. Schmidt, R.A. Pufahl, V.C. Culotta, T.V. O'Halloran, Undetectable intracellular free copper: the requirement of a copper chaperone for superoxide dismutase, Science 284 (1999) 805–808.
[30] D. Huster, S. Lutsenko, The distinct roles of the N-terminal copper-binding sites in regulation of catalytic activity of the Wilson's disease protein, J. Biol. Chem. 278 (2003) 32212–32218.
[31] R. Portmann, M. Solioz, Purification and functional reconstitution of the human Wilson copper ATPase, ATP7B, FEBS Lett. 579 (2005) 3589–3595.
[32] P.A. Cobine, G.N. George, C.E. Jones, W.A. Wickramasinghe, M. Solioz, C.T. Dameron, Copper transfer from the Cu(I) chaperone, CopZ, to the repressor, Zn(II)CopY: metal coordination environments and protein interactions, Biochemistry 41 (2002) 5822–5829.
[33] G. Multhaup, D. Strausak, K.D. Bissig, M. Solioz, Interaction of the CopZ copper chaperone with the CopA copper ATPase of *Enterococcus hirae* assessed by surface plasmon resonance, Biochem. Biophys. Res. Commun. 288 (2001) 172–177.
[34] A.K. Mandal, Y. Yang, T.M. Kertesz, J.M. Arguello, Identification of the transmembrane metal binding site in Cu+-transporting PIB-type ATPases, J. Biol. Chem. 279 (2004) 54802–54807.
[35] I. Voskoboinik, J. Mar, D. Strausak, J. Camakaris, The regulation of catalytic activity of the Menkes copper-translocating P-type ATPase. Role of high affinity copper-binding sites, J. Biol. Chem. 276 (2001) 28620–28627.
[36] R. Tsivkovskii, B.C. MacArthur, S. Lutsenko, The Lys1010-Lys1325 fragment of the Wilson's disease protein binds nucleotides and interacts with the N-terminal domain of this protein in a copper-dependent manner, J. Biol. Chem. 276 (2001) 2234–2242.
[37] E. Carafoli, The calcium pumping ATPase of the plasma membrane, Annu. Rev. Physiol. 53 (1991) 531–547.
[38] H.K. Simmerman, L.R. Jones, Phospholamban: protein structure, mechanism of action, and role in cardiac function, Physiol. Rev. 78 (1998) 921–947.
[39] P. Morsomme, M. Boutry, The plant plasma membrane H(+)-ATPase: structure, function and regulation, Biochim. Biophys. Acta 1465 (2000) 1–16.